High throughput near infrared screening discovers DNA-templated silver clusters with peak fluorescence beyond 950 nm

Journal:	*Nanoscale*
Manuscript ID	NR-COM-07-2018-005781.R1
Article Type:	Communication
Date Submitted by the Author:	25-Sep-2018
Complete List of Authors:	Swasey, Steven; UCSB, Chemistry and Biochemistry Copp, Stacy; Los Alamos National Laboratory, Center for Integrated Nanotechnologies Nicholson, Hunter; UCSB, Physics Gorovits, Alexander; University at Albany College of Computing and Information, Computer Science Bogdanov, Petko; University at Albany College of Computing and Information, Computer Science Gwinn, Elisabeth; UCSB,

Journal Name

COMMUNICATION

High throughput near infrared screening discovers DNA-templated silver clusters with peak fluorescence beyond 950 nm

Received 00th January 20xx,
Accepted 00th January 20xx

DOI: 10.1039/x0xx00000x

www.rsc.org/

Steven M. Swasey,[a] Stacy M. Copp,[b] Hunter C. Nicholson,[c] Alexander Gorovits,[d] Petko Bogdanov[d] and Elisabeth G. Gwinn*[c]

We use high throughput near-infrared (NIR) screening technology to discover abundant new DNA-stabilized silver clusters, Ag_N-DNA, that fluoresce in the NIR. These include the longest wavelength Ag_N-DNA fluorophores identified to date, with peak emission beyond 950 nm that extends into the NIR II tissue transparency window, and the highest silver content.

Many types of fluorophores are under development[1,2,3] to exploit the near-infrared (NIR) imaging windows in biological tissues,[4,5] including lanthanide complexes,[2] organic dyes,[6,7] carbon nanotubes,[8] quantum dots,[9] thiolate gold clusters,[10,11] and fluorescent silver clusters templated by short DNA strands (Ag_N-DNA).[12] With lower autofluorescence and greater penetration compared to the NIR I window (650-950 nm), the NIR II (1000-1350 nm) offers much higher imaging contrast,[7,13] but the impact of this advantage has been limited by a dearth of useful fluorescent labels compared to the profusion of biocompatible probes spanning the visible spectrum. This lack is in part due to low availability of cost-effective NIR II detectors, remedied in recent years by the emergence of commercial InGaAs detectors. As shown here, integration of these detectors into high throughput instrumentation enables rapid discovery of new Ag_N-DNA with fluorescence extending into the NIR II.

Ag_N-DNA have attracted much attention due to the dependence of their fluorescence properties on the choice of DNA template.[14] This sequence sensitivity, together with high quantum yields and good solution stabilities in some cases,[15] has inspired diverse visible wavelength applications for Ag_N-DNA[16] that include imaging in biological tissue,[17] screening for telomere binding ligands[18] and use in molecular logic gates for detection of pathogenic bacterial genes.[19] But for the NIR, development of Ag_N-DNA has been impeded by a dearth of known templates. Currently there are only two reported templates for Ag_N-DNA with peak emission wavelengths, λ_{em}, above 800 nm.[12] More templates are known for the 750-800 nm range,[20] but far fewer than the hundreds of templates for visible-emitting Ag_N-DNA that were identified in studies of large sets of candidate DNA sequences.[21]

Recent work has attempted to uncover the relation of sequence to the visible wavelength properties of Ag_N-DNA by use of machine learning algorithms applied to large data sets, resulting in improved ability to design template sequences for visible emitting Ag_N-DNA.[21] One complexity of the sequence-color problem is that a given template may produce multiple Ag_N-DNA with different fluorescence colors, corresponding to different silver cluster sizes. This is an advantage in the search for new Ag_N-DNA that fluoresce in the NIR, as we show below.

To rapidly screen candidate DNA strands as templates for NIR Ag_N-DNA, we used a fluorescence microplate reader (Tecan Infinite Pro 200) that was modified to include an InGaAs photodetector and a set of 50 nm emission bandpass filters spanning 700 nm -1400 nm.[22] Data were corrected for the detector's spectral responsivity. A Xenon flashlamp and UV bandpass filters (280-320 nm) were used for universal excitation of all Ag_N-DNA *via* the DNA absorbance band.[23] Correct spectral dependences of the NIR microplate reader were verified using a NIR fluorescence spectrometer (HORIBA Jobin Yvon Fluorolog®-3 with an InGaAs detector).

Three different 384 well microplates containing 844 unique DNA sequences, 10 -16 bases long, were studied using the rapid measurement capabilities of the NIR microplate reader. Each microplate well contained 30 µl samples of 375 (Plate A), 374 (Plate B) or 95 (Plate C) unique DNA strands originally selected as candidate templates for studies of the correlation between sequence and visible wavelength colors of Ag_N-DNA.[24] Synthesis was performed by robotic pipetting into the microplates by first

[a] Department of Chemistry and Biochemistry, UCSB, Santa Barbara CA, 93106
[b] Center for Integrated Nanotechnologies, Los Alamos National Laboratories, Los Alamos, NM 87545
[c] Physics Department, UCSB, Santa Barbara CA, 93106, USA. E-mail bgwinn@ucsb.edu
[d] Department of Computer Science, University at Albany, SUNY, Albany NY 12222
Electronic Supplementary Information (ESI) available: NIR spectra of selected unpurified samples, HPLC chromatograms, and sequences for the templates that produced emission with intensity-weighted emission wavelengths longer than 750 nm. See DOI: 10.1039/x0xx00000x

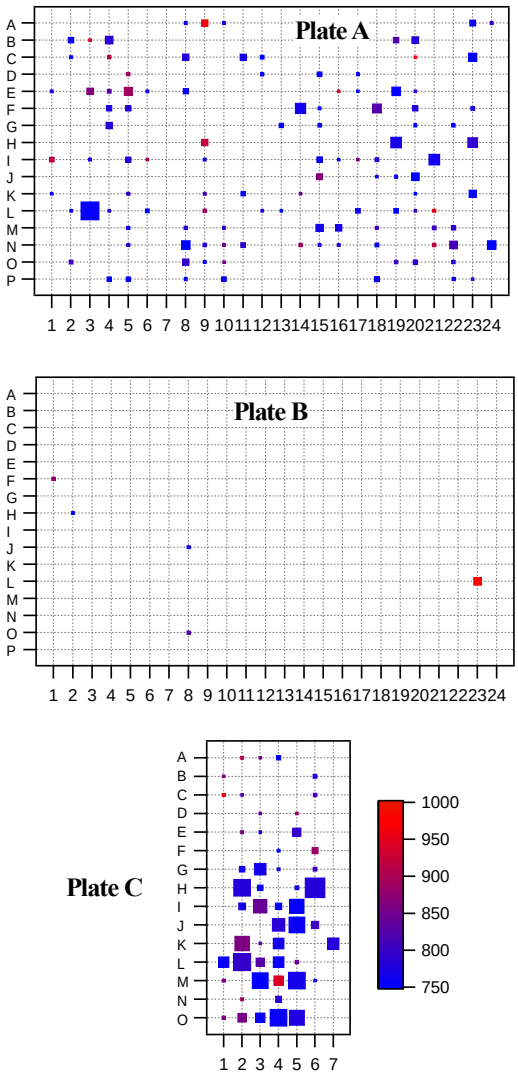

Fig. 1 NIR emission from Ag_N-DNA formed in three separate 384-well microplates containing a total of 844 unique DNA strands. Wells for which <λ> exceeds 750 nm are marked by squares with sizes that indicate integrated spectral intensity (Color bar for <λ> is at the lower right). Axes denote the well location of each template by row letter and column number. UV excitation (280-320nm). Plates A, B and C contained 375, 374 and 95 DNA templates, respectively.

mixing the DNA with $AgNO_3$ in NH_4OAc buffer (pH 7), then adding $NaBH_4$ after 17 minutes equilibration time. Final solution conditions were 20 μM DNA, 0.7 $AgNO_3$/base, 10 mM NH_4OAc and 0.5 $NaBH_4$:$AgNO_3$. We measured NIR emission spectra two weeks after synthesis to allow decay of unstable products.

Figure 1 summarizes the NIR results for the three microplates, with well location denoted by row letter and column number. Wells with intensity-weighted average emission wavelengths, <λ>, beyond 750 nm are marked with colored squares (wavelength color bar is at the lower right). Sizes of squares represent relative emission intensities.

As shown in Fig. 1, this rapid microplate format for NIR fluorescence characterization enabled discovery of more than 160 new DNA templates for NIR-emitting silver clusters (Table S1 lists sequences and properties). Apparently fluorescent NIR Ag_N-DNA are not intrinsically rare, and relatively few have been discovered previously simply due to lack of NIR characterization. Of the templates in plate A, which were designed to produce silver clusters that emit at wavelengths longer than 660 nm,[24] 30% also (or instead) stabilize Ag_N-DNA with <λ> beyond 750 nm, and 8% produce <λ> beyond 800 nm. In contrast, less than 2% of the templates in Plate B, which were designed to form clusters that emit in a shorter wavelength band (600-660 nm), give <λ> beyond 750 nm. Apparently NIR Ag_N-DNA are more likely to form on sequences designed as templates for clusters that emit at longer visible wavelengths. This finding is consistent with results for plate C, where the large number of NIR-emitting wells reflects selection of 75 templates, out of 1800 previously characterized at visible wavelengths,[21,24] for which silver cluster synthesis produced brightest emission beyond 700 nm.

Prior visible wavelength studies found that in many cases the fluorescent products formed by silver cluster synthesis on DNA templates are too fragile to isolate.[14] To identify robust Ag_N-DNA for the NIR, we selected ten candidate templates from the microplates in Fig. 1 based on the brightness and wavelengths of their NIR fluorescence, and optimized synthesis conditions to prepare sufficient material for separation by high performance liquid chromatography (HPLC). (Figure S1 shows sequences and NIR spectra of the unpurified samples). We used ion-pairing, reverse phase HPLC with 35 mM triethylamine ammonium acetate in the aqueous and methanol running buffers, and a 1-40% methanol gradient for all samples.

To determine the HPLC elution time for NIR-emitting Ag_N-DNA products, we developed a custom optical system to measure NIR emission in-line with the HPLC instrument, using a flow cell coupled to an InGaAs detector (Thorlabs, PDF10C, 800-1700 nm) via an 800 nm longpass filter. A 270 nm UV LED (Ocean
Optics) was used in pulse mode as the excitation source. A pulse generator (Hewlett Packard, 8116A) provided the pulse signal for the UV LED and a lockin amplifier (Stanford Research Systems, SR830 DSP) used to enhance the signal from the InGaAs detector. The signal from the lockin was output to an analog-to-digital converter (Measurement Computing, USB-1608G), recorded on TracerDAQ software and time-aligned with the simultaneously monitored DNA absorbance at 260 nm (Hitachi L-4200 UV/Vis detector) to form absorbance and NIR fluorescence chromatograms. After identifying the elution peak of the main NIR-emitting product for each sample, a second round of HPLC was performed to capture the purified product.

Of the ten DNA templates tested, half produced NIR Ag_N-DNA stable enough to withstand HPLC purification. Three of these exhibited emission peak wavelengths beyond 950 nm, listed in Table 1 with the template sequences and peak absorb-

Table 1. Properties of HPLC-purified Ag_N-DNA with peak emission wavelengths, λ_{em}, above 950 nm. (Spectra in Fig. 2).

Name	Sequence	λ_{em} (nm)	λ_{abs} (nm)
Ag_N-DNA 953	CGCCCCCACGCGCGGC	953 ± 2	854
Ag_N-DNA 962	ACACGAACCG	962 ± 3	687
Ag_N-DNA 999	CCTGGCCGGA	999 ± 4	685

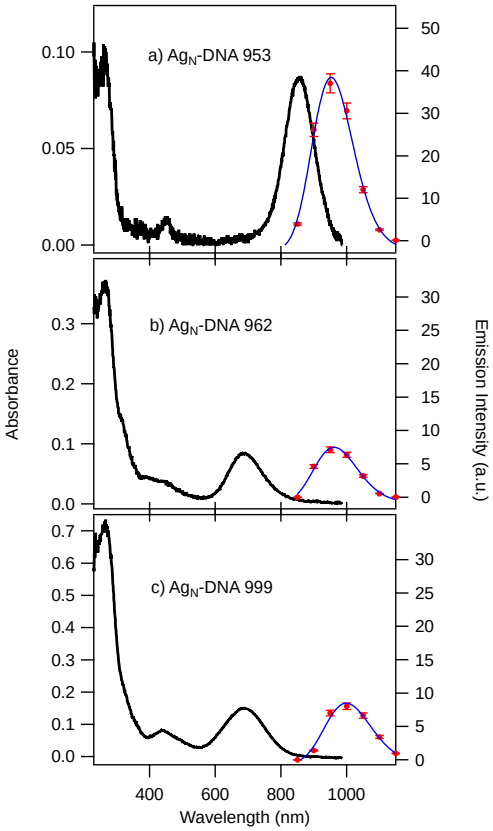

Fig. 2 Absorbance (black) and emission (red points) spectra for purified solutions of the Ag_N-DNA with emission maxima beyond 950 nm for a) Ag_N-DNA 953, b) Ag_N-DNA 962 and c) Ag_N-DNA 999. The emission spectra were excited in the UV using a Xenon flashlamp with 280-320 nm excitation bandpass filters.[22] Blue curves: Gaussian fits to the NIR fluorescence data points (red).

ance wavelengths. Emission and absorbance chromatograms measured during HPLC are shown in Fig. S2.

These are the longest wavelength Ag_N-DNA fluorophores identified to date. Ag_N-DNA 953 (Fig. 2a) is the main NIR product for the 16 base template in Table 1 (Fig. S2). Analysis of the absorbance and NIR fluorescence chromatograms (Fig. S3) indicates that Ag_N-DNA 953 was isolated in 74% purity. Ag_N-DNA 962 and Ag_N-DNA 999 are templated by shorter, 10 base strands (Table 1) and had much shorter elution times that precluded making quantitative purity estimates, though purity was improved by removal of slower-eluting products that were not fluorescent in the NIR (Fig. S2).

Figure 2 shows the absorbance and NIR emission spectra of the HPLC-purified samples Ag_N-DNA 953, Ag_N-DNA 962 and Ag_N- DNA 999. Gaussian fits (blue lines) to the emission data (red points, with instrumental error bars for the NIR fluorescence microplate reader) established the peak emission wavelengths in Table 1 (error bars are standard errors of the fit).

As shown in Fig. 2, these Ag_N-DNA have fluorescence extending beyond 1000 nm, into the NIR II window. For Ag_N-DNA 953 we obtain a fluorescence quantum yield (QY) of 7% through comparison of absorbance and NIR emission data to

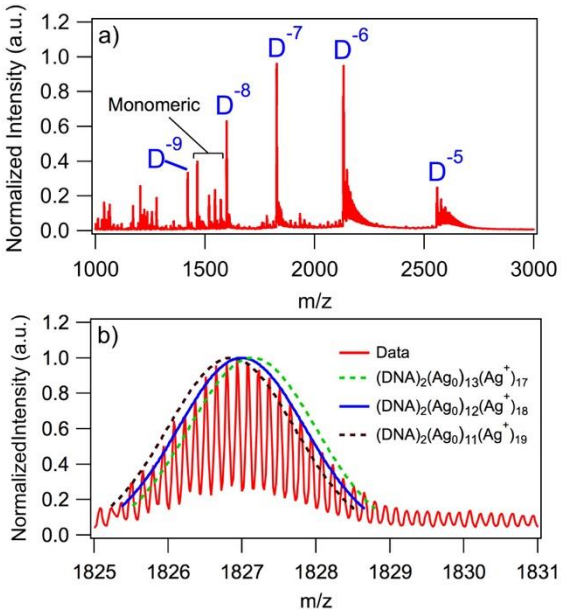

Fig. 3 a) Mass spectrum of the HPLC purified Ag_N-DNA 953. Peaks labelled "D^{z-}", where z is the charge state, contain two DNA strands and 30 Ag atoms. (The marked monomeric peaks contain one DNA strand. See Fig. S4 for more detail). b) ESI-MS data (red) and Gaussian fits to calculated isotope peak envelopes for products with various charges on the total silver content. Best agreement is for $(DNA)_2(Ag^0)_{12}(Ag^+)_{18}$.

the dye IR-125.[25] This compares favourably to other NIR fluorophores such as polymer-sorted single walled carbon nanotubes[26] (QY 2-3%) and the FDA-approved organic dye indocyanine green (ICG) (QY 0.9%),[7] and is similar to QY of heat optimized, thiolate gold clusters.[10]

Emission peak wavelengths of visible spectrum Ag_N-DNA have been found to correlate with the silver cluster size, specifically the number of neutral silver atoms (Ag^0).[14,27] Since little is known about composition of NIR Ag_N-DNA, we conducted electrospray-ionization mass spectrometry (ESI-MS) analysis on Ag_N-DNA 953, which was isolated in high enough purity to permit identification of composition and has the longest peak absorbance wavelength currently known for an Ag_N-DNA. Figure 3a displays the mass spectrum, which identifies a composition of 30 silver atoms holding two DNA strands together. (Such clusters that pair DNA strands are a common occurrence for Ag_N-DNA.[14,27]) By fitting the isotope peak envelope[14] we determined that 18 of the silver atoms are cationic (Ag^+), leaving 12 Ag^0 available to form a metallically bonded cluster.

This is the largest silver content yet identified for an Ag_N-DNA, both in neutral (Ag^0) and total silver content, and extends the previously established correlation[14] of peak wavelength to number of Ag^0 deeper into the NIR, at an even

number of Ag^0 consistent with the expectation for even magic number cluster sizes. [27] Apparently the formation of deep NIR clusters is not impeded by possible size limits that might arise from competition of DNA *versus* cluster length and energy scales.

Compared to the 99 nm Stokes shift of Ag_N-DNA 953, the much larger Stokes shifts of 275 nm for Ag_N-DNA 962 and 314 nm for Ag_N-DNA 999 indicate that they are structured differently, as do their much shorter HPLC elution times (Fig. S2). A large Stokes shift (211 nm) was also reported recently for a much shorter wavelength (λ_{em} = 736 nm) NIR I Ag_N-DNA.[28] The ESI-MS spectra (Fig. S5) show products with two DNA strands and 18-26 Ag atoms for Ag_N-DNA 962; and two DNA strands and 10-30 Ag atoms for Ag_N-DNA 999. Because the instrument-limited chromatogram peaks for Ag_N-DNA 962 and Ag_N-DNA 999 (Fig. S2) did not permit purity analysis, it is unknown whether the fluorescent silver cluster is the dominant product in the aliquot captured for ESI-MS, and therefore it is not possible to assign a composition.

By identifying Ag_N-DNA with emission extending into the NIR II, we have demonstrated the capabilities and importance of high-throughput methodology for discovery of longer wavelength NIR fluorophores. The narrow band, sequence-tuned fluorescence of Ag_N-DNA stands in qualitative contrast to the broad, featureless emission of NIR organic dyes such as ICG. Successful use of red-emitting Ag_N-DNA in earlier bioimaging studies[17] suggests that the NIR I – NIR II Ag_N-DNA reported here may prove useful as fluorescent labels for biological imaging. The discovery of many NIR templates from sequences originally designed to template deep red silver clusters indicates that inclusion of these new NIR Ag_N-DNA in future refinements of data-driven template design should enable further discovery of still larger silver clusters that fluoresce deeper into the NIR II.

The authors thank Monte Radeke for use of a pipetting robot acquired with support from NIH-NEI 5-R24-EY14799. This work was performed, in part, at the Center for Integrated Nanotechnologies, an Office of Science User Facility operated for the U.S. Department of Energy (DOE) Office of Science. Los Alamos National Laboratory, an affirmative action equal opportunity employer, is operated by Los Alamos National Security, LLC, for the National Nuclear Security Administration of the U.S. DOE under contract DE-AC52-06NA25396. S.M.C. acknowledges support from NSF-DGE-1144085. The DNA templates used in this work were supported by NSF-DMR-1309410 and the NIR instrumentation development was supported by NSF-CHE-1213895.

Conflicts of interest

There are no conflicts to declare.

Notes and references

1 J. Zhao, D. Zhong and S. Zhou, *J. Mater. Chem. B*, 2017, **6**, 349–365.

2 I. Martini, S. V Eliseeva and S. Petoud, *J. Lumin.*, 2016, **189**, 19–43.

3 A. Barbieri, E. Bandini, F. Monti, V. K. Praveen and N. Armaroli, *Top. Curr. Chem.*, 2016, **374**, DOI:10.1007/s41061-016-0048-9.

4 A. M. Smith, M. C. Mancini and S. Nie, *Nat. Nanotechnol.*, 2009, **4**, 710–711.

5 S. L. Jacques, *Phys. Med. Biol.*, 2013, **58**, 5007–5008.

6 Z. Starosolski, R. Bhavane, K. B. Ghaghada, S. A. Vasudevan, A. Kaay and A. Annapragada, *PLoS One*, 2017, **12**, 1–14.

7 J. A. Carr, D. Franke, J. R. Caram, C. F. Perkinson, M. Saif, V. Askoxylakis, M. Datta, D. Fukumura, R. K. Jain, M. G. Bawendi and O. T. Bruns, *Proc. Natl. Acad. Sci.*, 2018, **115**, 4465–4470.

8 M. Yudasaka, Y. Yomogida, M. Zhang, T. Tanaka, M. Nakahara, N. Kobayashi, Y. Okamatsu-Ogura, K. Machida, K. Ishihara, K. Saeki and H. Kataura, *Sci. Rep.*, 2017, **7**, 1–12.

9 J. Sun, M.-Q. Zhu, K. Fu, N. Lewinski and R. A. Drezek, *Int. J. Nanomedicine*, 2007, **2**, 235–40.

10 C. V. Conroy, J. Jiang, C. Zhang, T. Ahuja, Z. Tang, C. A. Prickett, J. J. Yang and G. Wang, *Nanoscale*, 2014, **6**, 7416–7423.

11 A. Mathew and T. Pradeep, *Part. Part. Syst. Charact.*, 2014, **31**, 1017–1053.

12 J. T. Petty, C. Fan, S. P. Story, B. Sengupta, M. Sartin, J.-C. Hsiang, J. W. Perry and R. M. Dickson, *J. Phys. Chem. B*, 2011, **115**, 7996–8003.

13 K. Welsher, S. P. Sherlock and H. Dai, *Proc. Natl. Acad. Sci.*, 2011, **108**, 8943–8948.

14 D. Schultz, K. Gardner, S. S. R. Oemrawsingh, N. Markeševič, K. Olsson, M. Debord, D. Bouwmeester and E. Gwinn, *Adv. Mater.*, 2013, **25**, 2797–2803.

15 E. G. Gwinn, D. E. Schultz, S. M. Copp and S. M. Swasey, *Nanomaterials*, 2015, **5**, 180–207.

16 Z. Yuan, Y.-C. Chen, H.-W. Li and H.-T. Chang, *Chem. Commun. (Camb).*, 2014, **50**, 9800–15.

17 Y. Antoku, J. Hotta, H. Mizuno, R. M. Dickson, J. Hofkens and T. Vosch, *Photochem. Photobiol. Sci.*, 2010, **9**, 716–21.

18 R. Cheng, J. Xu, X. Zhang, Z. Shi, Q. Zhang and Y. Jin, *Sci. Rep.*, 2017, **7**, 1–9.

19 J. Deng, Z. Tao, Y. Liu, X. Lin, P. Qian, Y. Lyu, Y. Li, K. Fu and S. Wang, *Chem. Commun.*, 2018, **54**, 3110–3113.

20 B. Sengupta, C. Corley, K. Cobb, A. Saracino and S. Jockusch, *Molecules*, 2016, **21**, 1–15.

21 S. M. Copp, P. Bogdanov, M. Debord, A. Singh and E. Gwinn, *Adv. Mater.*, 2014, **26**, 5839–45.

22 S. M. Swasey, H. C. Nicholson, S. M. Copp, P. Bogdanov, A. Govoritz and E. G. Gwinn, *Rev. Sci. Instruments*, 2018, accepted.

23 P. R. O'Neill, E. G. Gwinn and D. K. Fygenson, *J. Phys. Chem. C*, 2011, **115**, 24061–24066.

24 S. M. Copp, A. Govorits, S. M. Swasey, P. Bogdanov and E. G. Gwinn, *ACS Nano*, 2018, **12**, 8240–8247.

25 K. Rurack and M. Spieles, *Anal. Chem.*, 2011, **83**, 1232–1242.

26 A. Graf, Y. Zakharko, S. P. Schießl, C. Backes, M. Pfohl, B. S. Flavel and J. Zaumseil, *Carbon N. Y.*, 2016, **105**, 593–599.

27 S. M. Copp, D. Schultz, S. Swasey, J. Pavlovich, M. Debord, A. Chiu, K. Olsson and E. Gwinn, *J. Phys. Chem. Lett.*, 2014, **5**, 959–963.
28 S. A. Bogh, M. R. Carro-temboury, C. Cerretani, S. M. Swasey, S. M. Copp, E. G. Gwinn and T. Vosch, *Methods Appl. Fluoresc.*, 2018, **6**, 024004.

Microplate of candidate templates for NIR Ag_N-DNA

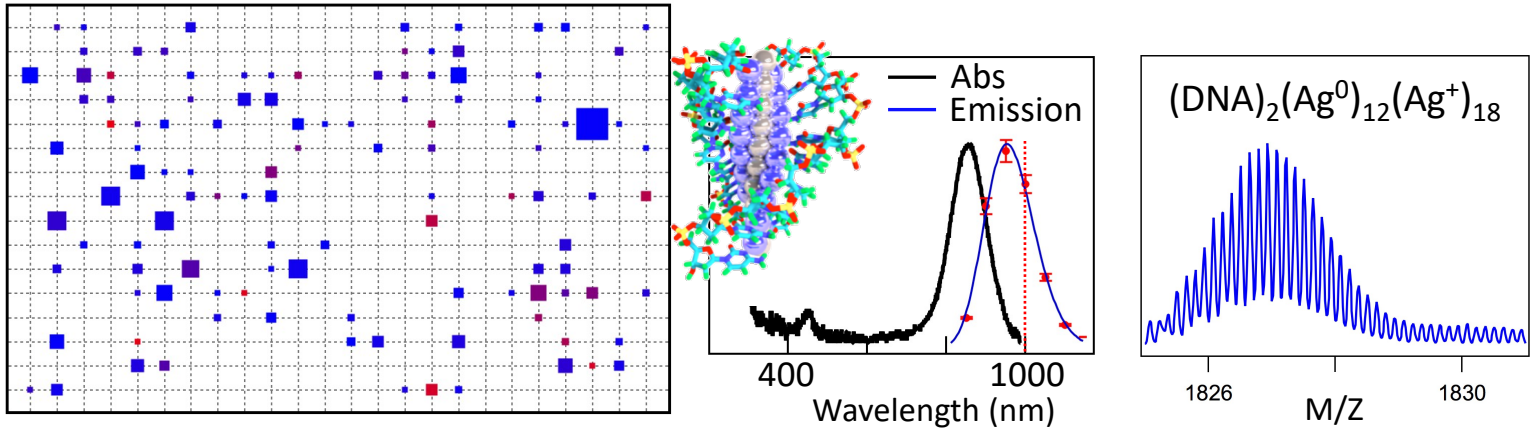

Table of Contents text: High throughput near infrared screening technology discovers DNA-stabilized silver clusters with fluorescence beyond 1000 nm.